Journal of Instrumentation

High-voltage pulsed generators for electro-discharge technologies

To cite this article: B M Kovalchuk *et al* 2013 *JINST* **8** P09012

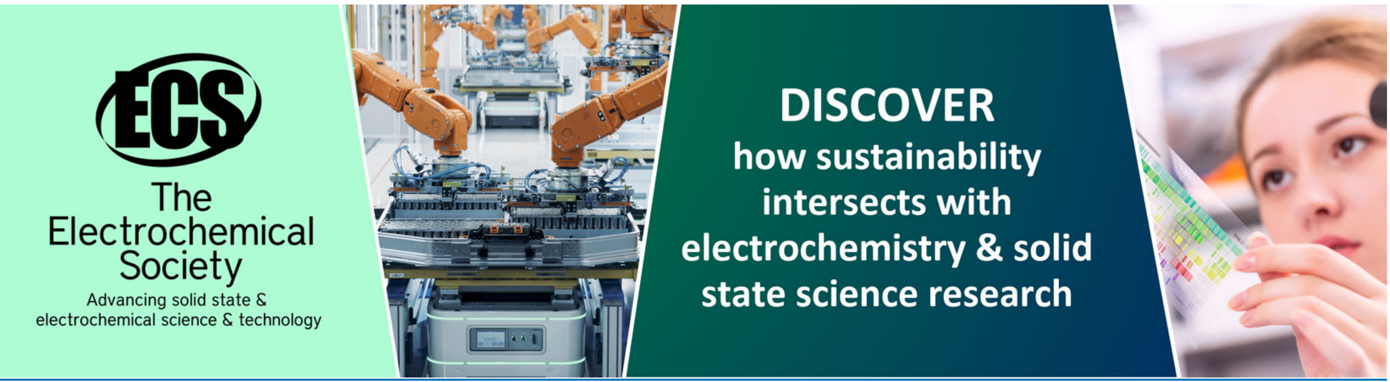

PUBLISHED BY IOP PUBLISHING FOR SISSA MEDIALAB

RECEIVED: *July 11, 2013*
ACCEPTED: *August 19, 2013*
PUBLISHED: *September 23, 2013*

High-voltage pulsed generators for electro-discharge technologies

B.M. Kovalchuk, A.V. Kharlov,[1] E.V. Kumpyak and V.A. Sinebrykhov

Institute of High Current Electronics,
Tomsk, 634055, Russia

E-mail: akharlov@lef.hcei.tsc.ru

ABSTRACT: A high-voltage pulse technology is one of effective techniques for the disintegration and milling of rocks, separation of ores and synthesized materials, recycling of building and elasto-plastic materials. We present here the design and test results of two portable HV pulsed generators, designed for materials fragmentation, though some other technological applications are possible as well. Generator #1 consists of low voltage block, high voltage transformer, high voltage capacitive storage block, two electrode gas switch, fragmentation chamber and control system block. Technical characteristics of the #1 generator: stored energy in HV capacitors can be varied from 50 to 1000 J, output voltage up to 300 kV, voltage rise time ~ 50 ns, typical operation regime 1000 pulses bursts with a repetitive rate up to 10 Hz.

Generator #2 is made on an eight stages Marx scheme with two capacitors (100 kV–400 nF) per stage, connected in parallel. Two electrode spark gap switches, operated in atmospheric air, are used in the Marx generator. Parameters of the generator: stored energy in capacitors $2 \div 8$ kJ, amplitude of the output voltage $200 \div 400$ kV, voltage rise time on a load $50 \div 100$ ns, repetitive rate up to 0.5 Hz. The fragmentation process can be controlled within a wide range of parameters for both generators.

KEYWORDS: Plasma generation (laser-produced, RF, x ray-produced); Pulsed power

[1]Corresponding author.

doi:10.1088/1748-0221/8/09/P09012

2013 JINST 8 P09012

Contents

1 Introduction

There has been an issue of interest for the last several decades in the use of high voltage (HV) pulse technology for rocks disintegration, because the electrical disintegration of rock through application of high voltage electrical pulses is one of the effective techniques in disintegration of mineral aggregates [1–4]. The experimental and theoretical studies on the applications of this technology were summarized by Semkin et al. [5, 6] for the time period of over 30 years. Main advantages of such technique are selectivity, high efficiency, and possibility of control in wide range of parameters [7–10]. This technique is also considered as an environment-friendly alternative to the use of explosives. An unique liberation process, involving the disintegration of ores by high voltage pulses has been suggested [11], as a possible route by which mineral liberation properties can be enhanced beyond conventional breakage methods. A report on the benefits to diamond liberation using high voltage pulses [12], suggested that diamonds liberated by pulses have no single mechanical defect and were cleanly detached from kimberlitic matrices. Mineral liberation by high voltage pulses and conventional comminution with the same specific energy levels was investigated recently [13, 14].

An electric breakdown strength of some liquids (including oil and water) can exceed the strength of solid materials at voltage pulse length below level of $\sim 1\,\mu$s [15, 16]. Indeed, for oil and water the electric breakdown strength is proportional to $\Delta t^{-1/3}$, while for solid dielectrics it is almost constant in the pulse length range 100 ns–10 μs. Therefore, in the nanosecond pulse regime of operation an increasing fraction of discharges is initiated through the solid, providing high efficiency of the fragmentation. Numerical simulation has been carried out [17] for minimization of the electrical energy consumption in an electric pulse fragmentation. Advanced physical and mathematical model of electro burst has been developed recently [18, 19]. Pulsed electric discharge heats the spark channel up to temperature $\sim 10^4$ K. The spark channel expands and launches a pressure wave (typically with amplitudes of 10^9–10^{10} Pa) into the surrounding solid material, leading to deformation and subsequent destruction of the material.

The most challenging aspects of this technology are both of electrical nature and mechanical engineering problems. The eventual use of multi-kJoule capacitor banks will put increased demands on the components of the system. The availability of long life time switches capable of commuting of high current at a repetition rate up to tens of Hz will become essential. Adequate protection mechanisms for the capacitors will also become an important issue since high energy density will be needed, and typically this type of device is sensitive to over-voltage stress.

Proper pulsed generator is key element in electric discharge technologies. Book [20] describes several designs of the generators for the rock fragmentation, recycling of building and elastoplastic materials, removal of surface layers, and drilling. Maxwell Physics International has developed and demonstrated a compact, transportable pulsed power-based system (100–200 kV, up to 3 Hz) for disaggregating rocks [21]. Self-contained, compact, semi-automated device [22, 23] was demonstrated by SELFRAG AG (Switzerland, the name of SELFRAG refers to selective fragmentation). The equipment consists of a high voltage power supply, a high voltage pulse generator (90–200 kV, up to 5 Hz), and portable treatment vessel.

Generator #1 can be considered as upgrade of prototype [24], but with enhanced energy and flexibility. Most of the devices for electro-pulse technology include a Marx generator for the formation of a high voltage pulse. Disadvantage of the Marx scheme is that large number of spark gaps is required with synchronous triggering. Described in this paper generator on 1 kJ consists of one HV storage, charged to full voltage, and one switch. This storage (capacitor bank) is pulsed charged from the pulsed transformer. Such solution simplifies design and enhances the system reliability.

Although the #2 generator is made on Marx scheme, custom design of a switch block ensures synchronous triggering. Generator #2 can be considered as one of the most powerful generators in the world, operating in continuous regime at 0.5 Hz frequency.

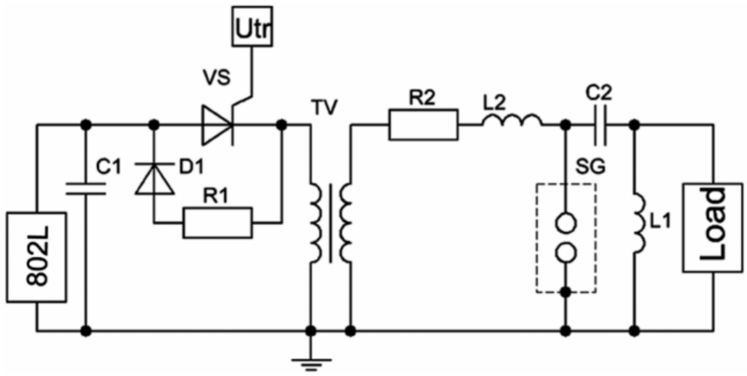

Figure 1. Principal electrical scheme of the generator.

2 Fragmentation generator #1 on 1 kJ

2.1 Operation principles

Principal electrical scheme of the generator is given in figure 1. At command from the control system the 802L power supply charges the C1 primary storage up to preset value 1.5–1.8 kV. After it triggering pulse Utr turns on the thyristor switch VS and energy from the primary storage C1 transfers through the HV transformer TV on the HV capacitor bank C2, charging it up to required value ($200 \div 300$ kV). L1 is a large charging inductance ($\sim 150\,\mu$H). Protective inductor L2 ($220\,\mu$H, $40\,\Omega$) damps oscillations, which appear after a main discharge. Amplitude of the current pulse from the low voltage block is ~ 15 kA with the pulse duration $\sim 120\,\mu$s. A circuit from the diode D1 (DF-453-800A-4600V) and resistor R1 ($0.1\,\Omega$) is installed in parallel with the thyristor. This circuit returns and absorbs the pulse energy that has not been delivered to a load.

At voltage close to maximum the gas switch SG breaks down and the HV capacitor bank C2 is discharged on a load. This process is repeated until acquisition of required pulse number.

2.2 Low voltage block

It incorporates HV power supply TDK-Lambda 802L-2KV-POS-400VAC (2 kV, 8 kJ/s), a primary capacitive storage C1, a thyristor switch VS, a demagnetization block, and an automatics block. The C1 capacitor bank is assembled from 128 connected in parallel capacitors ELECTRONICON E53 (2400 V, 4.7 μF, metalized film capacitors). The maximum charging voltage on C1 is +2 kV, and the maximum stored energy is 1200 J. The thyristor switch VS is made on fast thyristor TBI-193-2500A-3000V.

Automatics block consists of a power supply on 24 V, control contactors, triggering block, air conditioning system, relays and safety interlocks. The triggering block forms pulse Utr ~ 15 V for command to the thyristor switch. The demagnetization block converts core of a HV transformer to an initial magnetic state after each pulse. The demagnetization block supplies 70 A DC current that is continually flowing through a HV transformer primary winding. The air conditioning system provides filling of the gas switch by dry air, purge during operation and air exhaust after a shot burst.

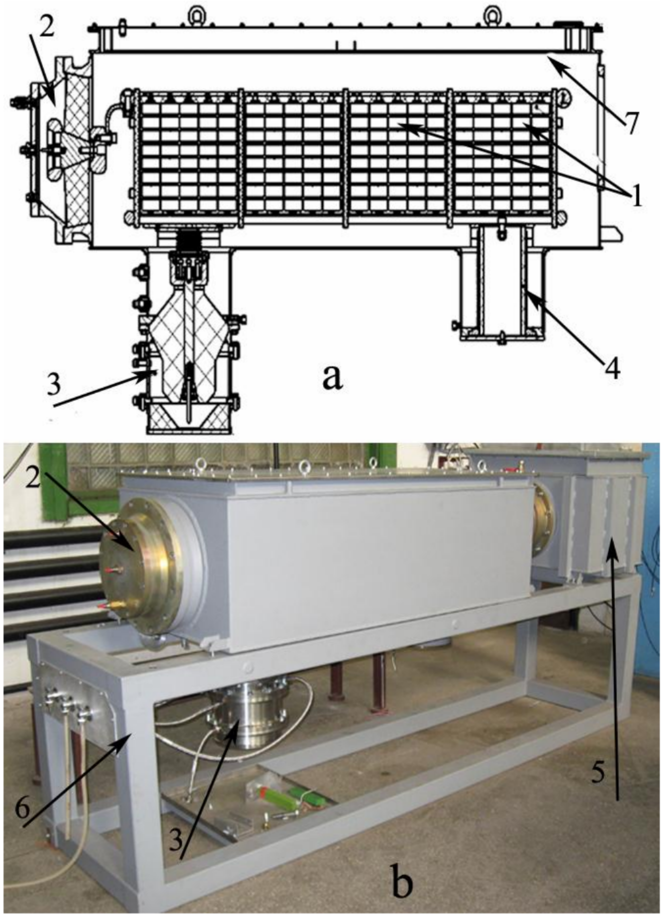

Figure 2. a: lengthwise section of the HV capacitive storage: 1 — capacitor blocks, 2 — spark gap, 3 — fragmentation chamber, 4 — charging inductor, 7 — plate of the capacitive divider; b: picture of the generator: 5 — block of the HV transformer, 6 — support.

2.3 Control system

It provides remote control of all blocks of the generator and measurements of the voltage and current on a treatment chamber. In particularly, the control system checks all devices and security contacts before authorizing the charging and shooting. The system also allows fine adjustment of the charging voltage and gas switch pressure. Controller block executes commands, received from a computer, and sends back to the computer status information about hardware of the generator. Controller block interacts with operated objects and measurement sensors through an interface block.

2.4 High voltage block

HV block consists of a HV transformer block and HV capacitive storage block, which are mounted on one frame (figure 2b). Block of the high voltage transformer is fixed immobile on the frame. Block of the HV capacitive storage is mounted on adjustable support and wheels that allows to disconnect it from the HV transformer block and move along the frame.

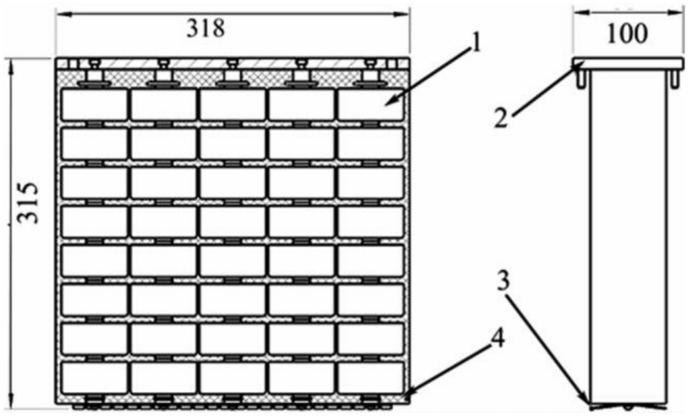

Figure 3. Assembling drawing of the capacitor block: 1 — capacitors UHV-12A, 2 — top mounting plate, 3 — Collet contact plate, 4 — body formed from epoxy compound.

2.4.1 HV capacitive storage block

Figure 2a shows assembling drawing of the HV capacitive storage block. It incorporates capacitor bank (1), capacitive voltage divider (7), charging inductor (4), gas switch (2) and fragmentation chamber (3). Capacitive storage is made as stacked frame from 20 capacitor blocks, placed in four sections. Capacitive bank is mounted in a metal tank, filled with transformer oil. Total capacitance of the battery is equal to 21.25 nF. Capacitance can be changed by disconnection of part of the capacitor blocks.

Design of the capacitor block is shown in figure 3. Each capacitor block consists of 40 ceramic capacitors type UHV-12A (1700 pF, 50 kV, TDK corporation). TDK UHV series high voltage ceramic disk capacitors feature low dissipation and excellent voltage-capacitance characteristics using strontium titanate for dielectric material. They are epoxy-encapsulated to meet requirement of high voltage applications. The block capacitors are assembled in series-parallel (5 stacks with 8 caps in stack) and molded in epoxy compound. Capacitors (1) are sealed off within epoxy in the block body permanently. Epoxy sealing both enhances external electric insulation of the capacitors and ensures mechanical strength of the capacitor block.

2.4.2 Block of a high voltage transformer

This block consists of HV pulsed transformer (2) and protecting inductor (3) (see figure 4). These HV block components are mounted in a metal tank (1), filled with transformer oil. Design of the bank allows vacuum pumping at filling of the bank with transformer oil in order to prevent air bubbling. Protective inductor 3 is intended for damping of oscillations, which appear at the switch firing. Transformer design is given elsewhere [24]. Main parameters of the transformer are summarized in table 1.

2.4.3 Fragmentation chamber

Design of the rock fragmentation chamber is shown in figure 5. Interface insulator (2) separates oil volume of the HV capacitive storage and volume of the fragmentation chamber. Current input electrode (1) is fixed in the insulator (2) with use of fastening element (5). Central electrode of

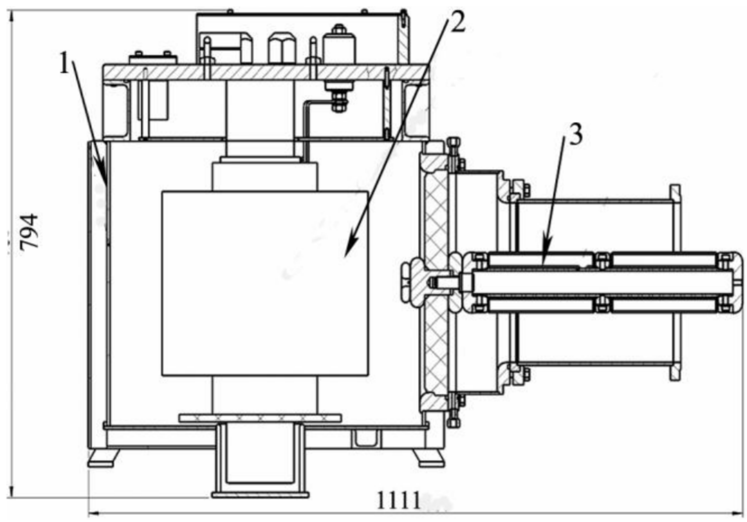

Figure 4. Lengthwise section of the high voltage transformer block: 1 — tank of the block; 2 — high voltage pulsed transformer; 3 — protective inductor.

Table 1. Main parameters of the transformer (at 500/1000 J in the output pulse).

Transformation coefficient	170
Current pulse length (half period)	$85/120\,\mu$s
Current amplitude on the primary	10.6/15.7 kA
Current amplitude on the secondary	60/90 A
Voltage amplitude on the secondary	330 kV
Resistance of the primary winding	0.5 mΩ
Resistance of the secondary winding	12 Ω
Energy loss per pulse in the core	7/15 J

the fragmentation chamber is connected to bottom plate of the HV capacitive storage through the flange (4). Bellows expansion joint (3) decouples mechanically flange (4) and fixing element (5). Treated material is placed in the conical cavity (11) of the insulator (8). Discharge occurs between electrodes (9) and (10) through a treated material. Vertical position of the electrode (9) could be adjusted through the spring (12). This spring also damps vibrations of the electrode (9), arising at discharge. All elements of the treatment chamber are made from the stainless steel, except insulator (2), which is made from polyethylene block. Treatment chamber has been tested at 3 bar pressure.

2.5 Tests of the #1 generator

2.5.1 Operation regimes of the generator

The generator was tested in two regimes, namely in regime with an active load equivalent and regime of rock fragmentation.

2013 JINST 8 P09012

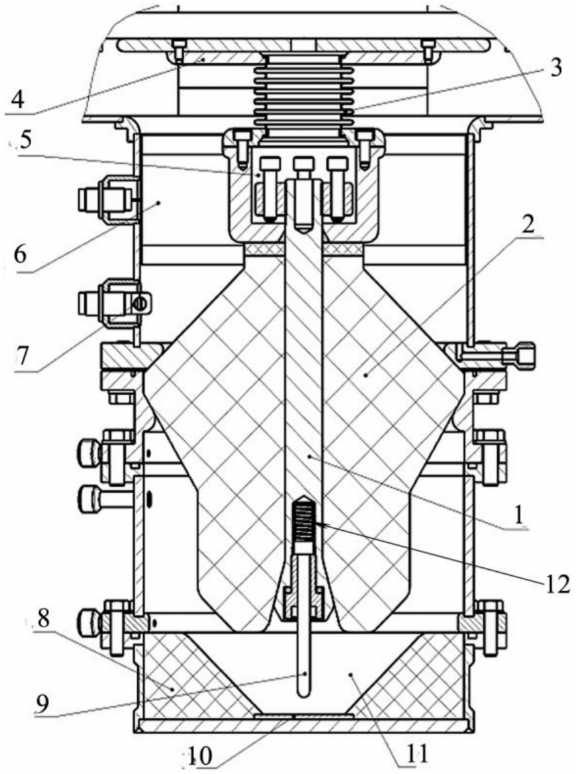

Figure 5. Chamber for rock fragmentation: 1 — current input electrode, 2 — interface insulator (oil-air), 3 — bellows expansion joint, 4 — flange, 5 — fixing element, 6 — capacitive voltage divider, 7 — current probe, 8 — insulator of the fragmentation chamber, 9 — HV electrode of the treatment chamber, 10 — ground electrode, 11 — cavity for material treatment, 12 — spring.

Active load equivalent. Load resistance in this regime is formed by water column between HV electrode and grounded flange of the fragmentation chamber. Dimensions of the electrodes and insulator are adjusted in order to get load resistance $\sim 40\,\Omega$. Appearance of the electrodes in the treatment chamber in the material fragmentation regime is shown in figure 5. In this case gap between HV electrode (9) and electrode (10) is equal to 10–15 mm. Tests of the generator have been performed at charging voltages 1.5 kV and 1.8 kV by 1000 shots bursts with 10 Hz frequency. At charging voltage 1.5 kV gap distance in the gas switch is equal to 18 mm, pressure in the switch volume is equal to 5.2 bar (absolute value). At charging voltage 1.8 kV gap distance in the gas switch is also equal to 18 mm, pressure in the switch volume is equal to 6 bar (absolute value). Jitter in breakdown voltage of the gas switch was about 5%.

2.5.2 Diagnostics

Diagnostic probes are similar to that described in prototype generator [24].

- Capacitive voltage divider monitors the charging voltage on the HV capacitor bank. The divider is made from coated fiberglass sheet ($1570 \times 680 \times 2\,\text{mm}^3$). High voltage leg of the divider is capacitance (~ 150 pF) between HV plates of capacitor blocks and surface of coated fiberglass sheet. Low voltage leg (between fiberglass sheet and ground) capacitance is

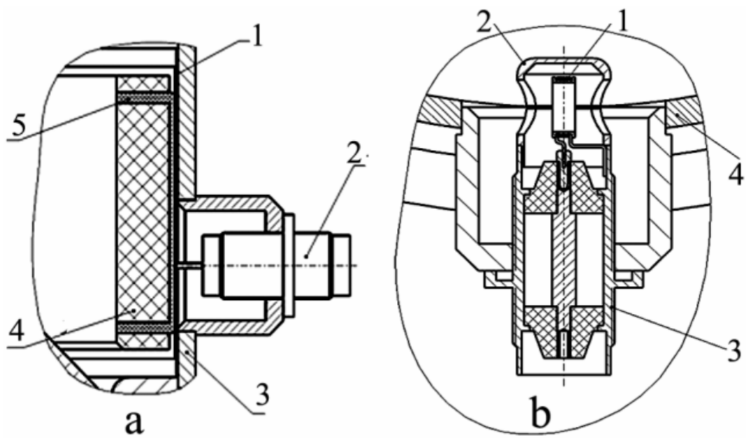

Figure 6. Diagnostics in the fragmentation chamber, a: design of the capacitive divider: 1 — coated fiberglass; 2 — vacuum sealed connector; 3 — body of the treatment chamber; 4 — polyethylene insert; 5 — rubber cord; b: design of shielded current probe: 1 — coil, 2 — metal shield, 3 — vacuum sealed connector, 4 — body of the fragmentation chamber.

27.9 nF. Additional resistor $R = 3,7\,\mathrm{k\Omega}$ is installed at the divider output in order to increase time constant of the divider. Time constant of the low voltage leg is $\sim 105\,\mu$s.

- Design of diagnostic probes in the fragmentation chamber is given in figure 6. Load voltage is monitored by capacitive divider (figure 6a). It is made from strip of coated fiberglass (width 90 mm and 0.5 mm thickness), mounted on the inner surface of the treatment chamber. Polyethylene insert (4) with rubber cords (5) fix the divider, providing tough contact with the chamber body. High voltage leg capacitance of the divider is capacitance between central electrode (pos. 1, figure 5) of the chamber and coated fiberglass strip. Capacitance C_{lv} of the low voltage leg of the divider is $\sim 5,99$ nF. Signal from the divider is taken out through vacuum sealed connector SRG-75. Additional resistor $R = 3,7\,\mathrm{k\Omega}$ is installed at the divider output in order to increase time constant of the divider. Time constant of the circuit $C_{lv} \times (R_c + R_t)$ is $\sim 22.5\,\mu$s, where $(R_c + R_t)$ — resistance of the measurement channel of the divider. Calibration of the capacitive voltage dividers has been performed with use of the active voltage divider.

- Load current is measured by inductive probe (figure 6b). The probe is made as coil (2), which is winded by $\varnothing\,0.6$ mm wire on the insulator rod $\varnothing\,10$ mm. Coil outputs are soldered to outputs of the vacuum sealed connector 3. Coil is enclosed by metal shield 2 in order to decrease capacitive coupling. Internal space inside shield is filled by epoxy compound.

2.5.3 Experimental results

Typical waveforms of the charging voltage on the HV capacitive storage are shown in figure 7 for two values of the stored energy, namely 500 and 1000 J. Voltage amplitude is about 290 kV for the charging voltages of 1.8 kV, charging time is larger on $\sim 20\,\mu$s at 1000 J in the capacitor bank. Traces of the load current and voltage are given in figure 8a,b for operation on load equivalent and

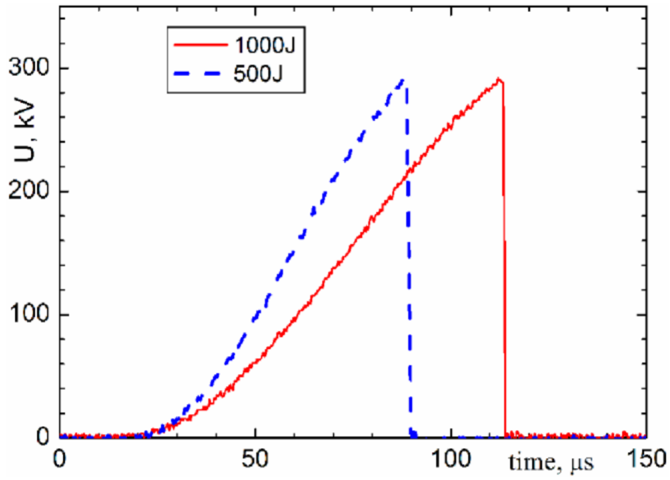

Figure 7. Voltage waveforms on the HV capacitive storage at 1.8 kV charging voltage on the primary storage with 500 and 1000 J stored energy.

Table 2. Summary of the generator tests results for rock load at 1.8 kV charging voltage.

Stored energy (J)	Charging time (μs)	Load voltage (kV)	Load current (kA)	Voltage rise time (ns)
250	55	330	~ 20	~ 50
500	75	350	~ 30	~ 50
1000	100	380	~ 50	~ 50

in rock fragmentation regime. Voltage and current on figure 7a exhibit exponential decay, typical for a discharge of the capacitance on the active load. Temporal behavior of the voltage and current is the same on the active load, and there is no delay between voltage and current.

Waveforms in the fragmentation regime (figure 7b) are quite different: there is a large voltage spike at the beginning of the pulse, then the voltage drops sharply (time moment of the complete breakdown) and the current rises. The current amplitude in the fragmentation regime is about five times larger, than in the active load regime. Figure 9a,b shows pictures of granite and concrete samples after treatment at 500 J, 10 Hz, 1000 pulses. Detailed investigation of the fragmentation processes was out of scope of our work table 2 shows main parameters of the generator operation depended on the stored energy at charging voltage of 1.8 kV.

2.6 Maintenance work

- Replace high voltage electrode of the gas switch (small cupper cylinder with diameter of 6 mm and length of 20 mm) at erosion material removal more than 0.5 mm ($\sim$ 30000 pulses). Also clean the switch insulator with gasoline at this time.
- Replace central rod electrode of the treatment chamber at erosion material removal more than 2 mm ($\sim$ 50000 pulses).

Replaceable parts are very cheap and $\sim$ 5 min is only needed for the replacement.

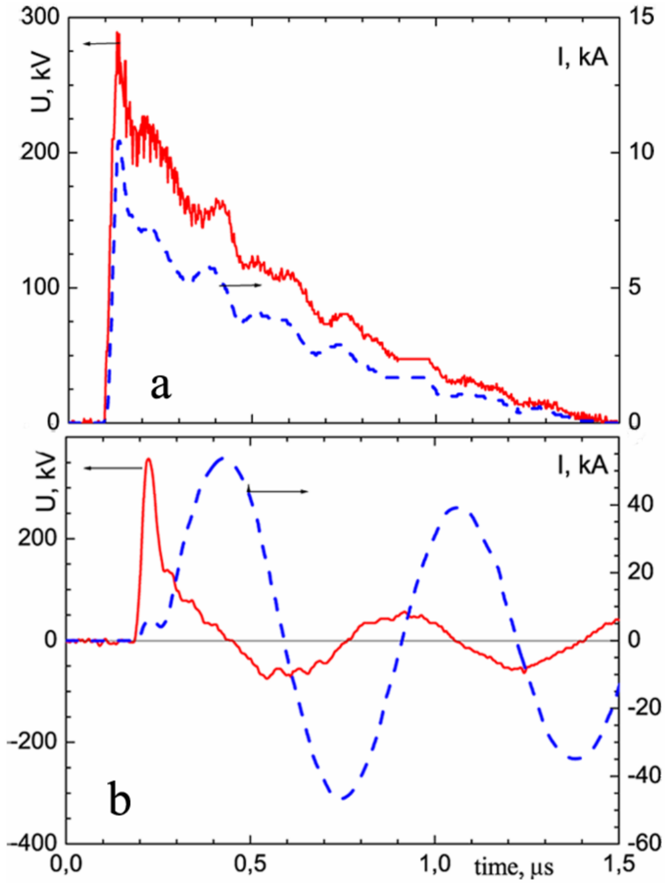

Figure 8. a: load voltage U and current I at operation on the load equivalent; b: at operation in rock fragmentation regime (charging voltage 1.8 kV, stored energy 1000 J).

3 Fragmentation generator #2 on 8 kJ

3.1 Operation principles

Block-scheme of the installation is given in figure 10. It consists of electrical cabinet and block of pulsed generator with fragmentation chamber. Electrical cabinet consists of the next blocks:

- High voltage power supply series 802L-50 kV LAMBDA — provides charging of the Marx capacitors.
- Pulse forming block — at firing of the generator provides signal to shot counter and through it to high voltage power supply.
- Shots counter — turns on high voltage, counts number of shots of the generator and turns off high voltage after required amount of shots.
- DUMP — element of safety system. Provides discharge of the Marx capacitors at end of operation or at emergency.

2013 JINST 8 P09012

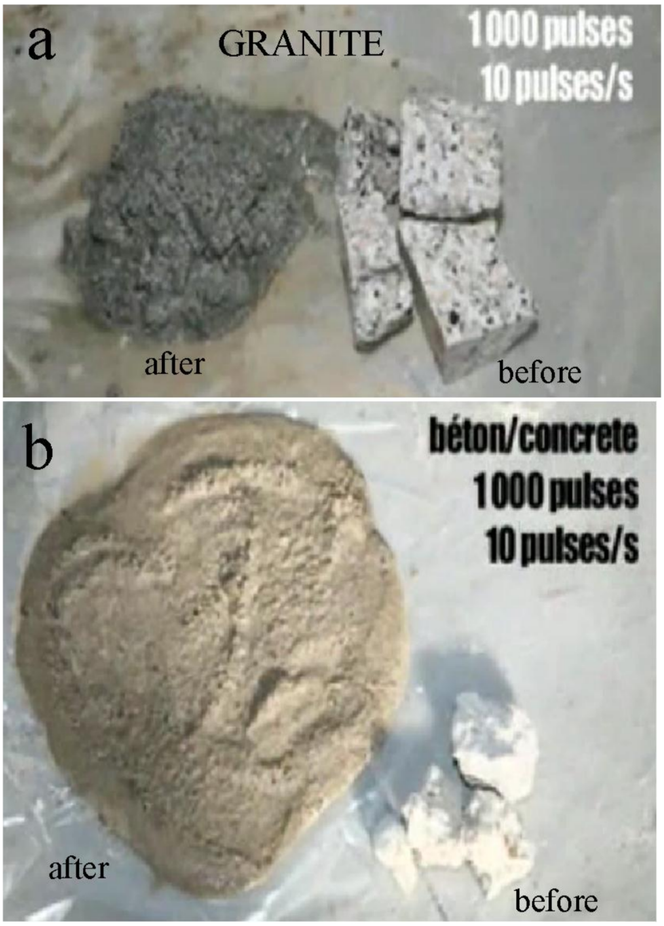

Figure 9. Fragmentation examples.

- Air conditioning system — provides filling of the switch block by dry air up to given value and air exhaust after shot burst.

All blocks and elements of the electrical cabinet are placed in metal box with dimensions $0.55 \times 0.55 \times 1.15\,\mathrm{m}^3$.

Blocks of the pulsed generator are mounted in a metal tank, filled with transformer oil. Marx generator, support insulator and transition insulator are installed in this tank. Fragmentation chamber is connected through the transition insulator. Pictures of the pulsed generators are given in figure 11.

The installation works in the following way: operator enters required charging voltage on the HV power supply, number of shots in burst on the counter, frequency of operation of the generator and pressure in the gas switch. At entering of the "Start" command the generator begins operation. HV Power supply charges capacitors of the Marx generator up to 25–50 kV in $\sim 0.2 \div 0.9$ s. At voltage rising to self-breakdown level the Marx switches break down and voltage pulse with amplitude $200 \div 400$ kV is delivered to the fragmentation chamber. Voltage and current waveforms on a load, registered by voltage dividers and inductive probe, are monitored by an oscilloscope.

2013 JINST 8 P09012

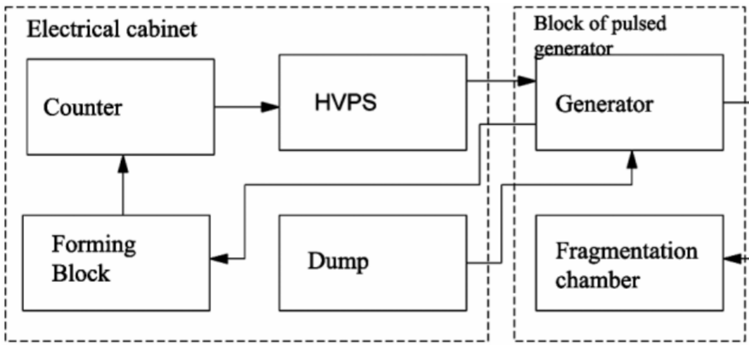

Figure 10. Block scheme of the generator.

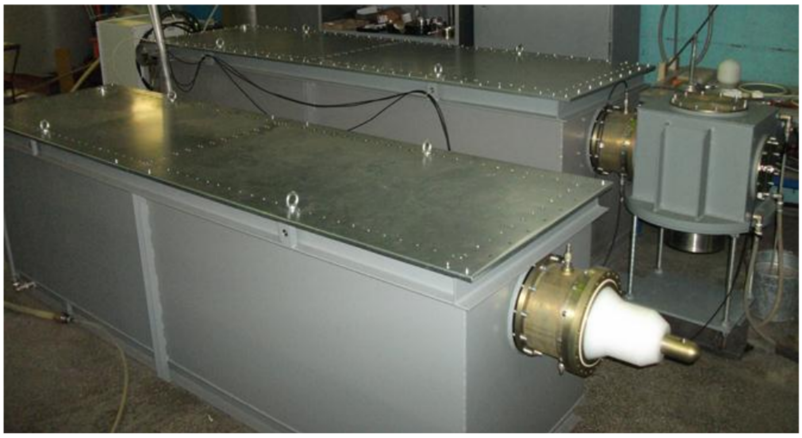

Figure 11. Picture of pulsed generators.

3.2 Marx generator

3.2.1 Principal scheme

Pulsed voltage generator #2 is made on the Marx scheme (see figure 12). There are 8 stages (C1-C8) in the generator, and each stage consists of two connected in parallel IK-100-0.4 capacitors. Maximum output voltage of the capacitor is 100 kV, capacitance 0.4 μF, inductance 140 nH. Despite nominal rated voltage of 100 kV for these capacitors, maximum charging voltage for operation of the Marx generator has been chosen as 50 kV in order to increase lifetime of the capacitors. Stages of the generator are charged through the charging inductors (L1-R1, L16-R16).

3.2.2 Marx design

Assembling drawing of the generator is given in figure 13. Capacitors of the stages (1) are mounted in the container (2). Container is made from plastic and bolted from one side to the generator body (8), the other side of the container is supported by the acrylic insulator (6). The switches block (3) with fastened to it charging inductors block (4) is placed above of the capacitors. Voltage from the generator body to the fragmentation chamber is delivered through the interface insulator (7). All stages of the generator are covered by aluminum shields (5) which are connected with low voltage terminals of the capacitors. Charging voltage to the stages capacitors is supplied by

2013 JINST 8 P09012

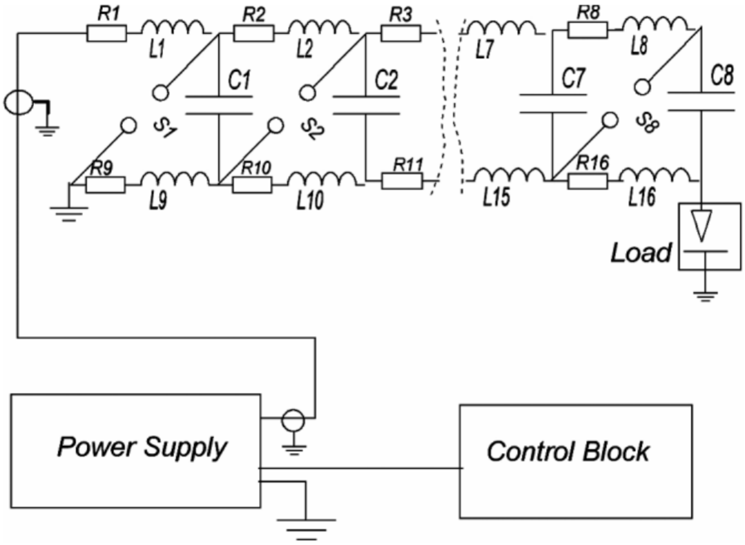

Figure 12. Principal electrical scheme of the #2 generator.

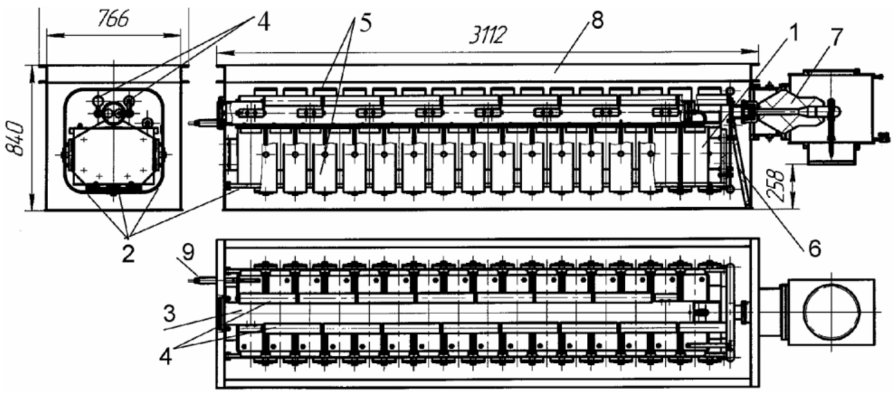

Figure 13. Generator #2 with fragmentation chamber: 1 — capacitors of the stages, 2 — container for capacitors, 3 — switch block, 4 — charging indictors, 5 — shields, 6 — support insulator, 7 — insulator of the fragmentation chamber, 8 — body of the generator, 9 — charging voltage input connector.

cable through HV connector (9). Volume of the generator is filled by transformer oil and covered by lid. There is some air gap under lid for compensation of oil inflation at temperature increase. Oil volume is $\sim 1.5\,\mathrm{m}^3$, weight of the generator $\sim 2.5\,\mathrm{t}$.

3.2.3 Switches of the Marx generator S1-S8

Two electrode spark gap switches, filled with dry air, are used in the generator. Self breakdown voltage of the gaps is adjusted by change of air pressure in the switches. All eight switches are mounted in one body from fiberglass tube, forming the switch block (figure 14b). Electrode system of gas switch is given in figure 14a. Electrodes (1) are fixed on the tube (3) by screws (5). Switch electrodes are made from copper with large surface in a discharge zone in order to decrease erosion of the electrodes. Charging inductors and capacitor terminals are connected to the contacts (2). Teflon o-rings (4) provide sealing of the switch block volume. Value of spark gap d is equal to

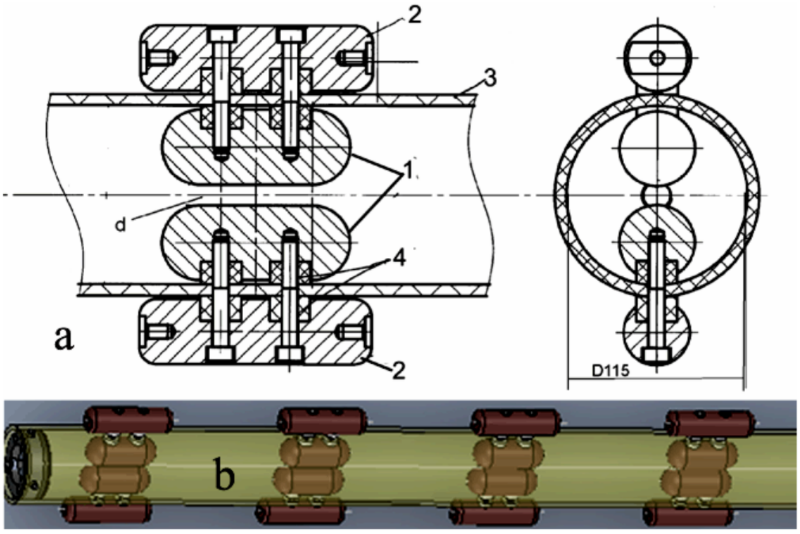

Figure 14. a: electrode system of gas switch: 1 — copper electrodes, d — spark gap, 2 — contacts for connection with capacitor, 3 — body, 4 — sealing o-ringes (teflon).

8 mm. Switch electrodes are made from copper. For protection from discharge byproducts inner surface of the switch body is covered by mylar film with 0.2 mm thickness.

3.2.4 Charging inductor

These inductors are made without magnetic core with inductance of 145 μH and active resistance of 29 Ω. The coil is winded by NiCr wire on a fiberglass tube. Such design provides high mechanical strength of the inductor. These inductors provide low energy loss at charging of the stage capacitors and limit current at level of 1.5–2 kA at the generator self firing (for example when there is no discharge between electrodes in the fragmentation chamber). Interior space of the Marx generator with placement and connections of the capacitors, switches and inductors is shown in figure 15.

3.3 Fragmentation chamber

Assembling drawing of the fragmentation chamber is given in figure 16. Fragmentation chamber is filled with water and has cavity for treated sample placement. Inductive current probe, active and capacitive voltage dividers are placed In the fragmentation chamber. Rectangular body (1) of the chamber is made from steel with dimensions $500 \times 400 \times 400\,\text{mm}^3$. Interface insulator (3) from polyethylene is installed in the cylinder (8), which connects the generator and fragmentation chamber. The insulator is fixed by the flange (2). Treated material is placed in the conical cavity of the insulator (6). The chamber is filled with water with some air gap at the top in order to decrease hydraulic shock on the walls. Discharge occurs between electrodes (5) and (7) through the treated material. Capacitive voltage divider and inductive current probe are installed in the cylinder (9). Load voltage after breakdown is measured by active voltage divider 12.

2013 JINST 8 P09012

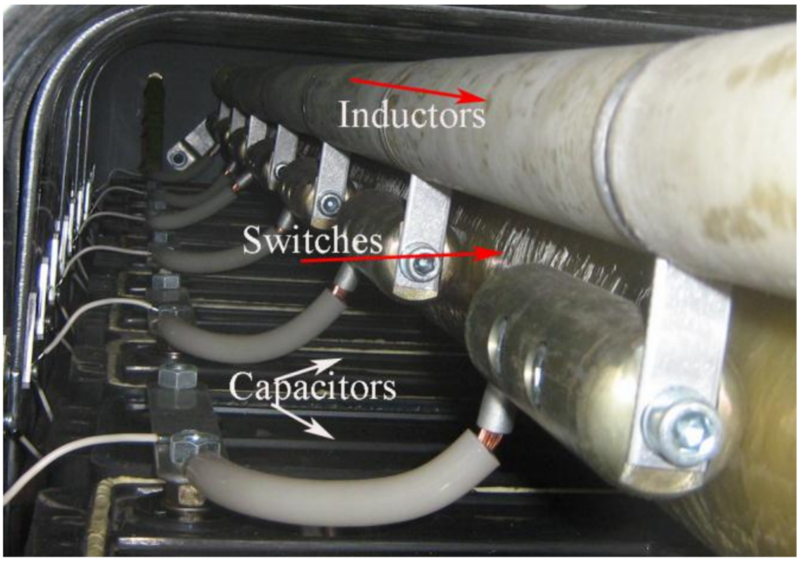

Figure 15. Connection of the capacitors, switches and inductors.

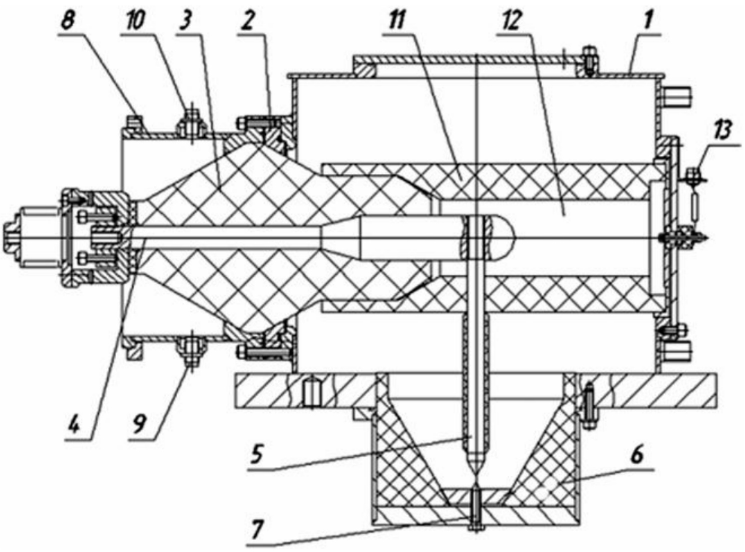

Figure 16. Fragmentation chamber: 1 — body, 2 — flange, 3 — insulator, 4 — high voltage input, 5 — HV electrode, 6 — insulator of the fragmentation cavity, 7 — low voltage electrode, 8 — transitive cylinder, 9, 10, — probes, 12 — voltage divider.

4 Tests of the #2 generator

The generator was also tested in two regimes: on active load equivalent ($\sim 8\,\Omega$) and regime of rock fragmentation. Appearance of the electrodes in the treatment chamber in the material fragmentation regime is shown in figure 15. In this case gap between HV electrode 5 and electrode 7 is equal to 20 mm.

Tests of the generator have been performed at pressure in the switches of 1, 1.5, 2, 2.5 and 3 bars (absolute value). Self breakdown values at these pressures were 20, 26, 32, 39 and 45 kV,

2013 JINST 8 P09012

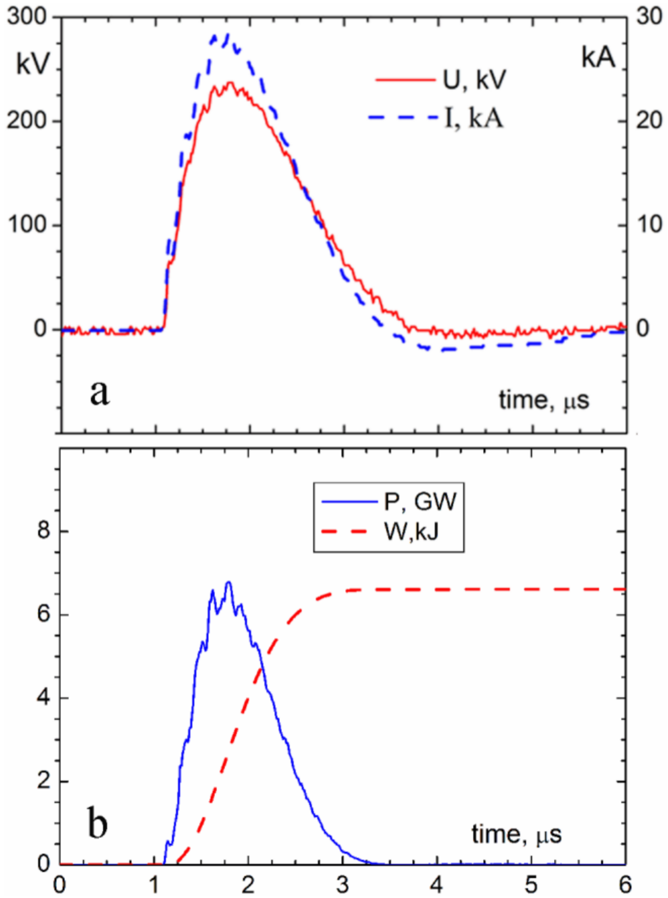

Figure 17. a: waveforms of load voltage U and current I; b: calculated curves for power P and energy W for the load equivalent regime at charging voltage 45 kV.

respectively. Traces of the load current, voltage, and calculated curves for power and energy are given in figure 17a,b for operation on a load equivalent. Voltage and current waveforms on figure 16a exhibit behavior close to critical damping discharge of an R-L-C circuit. It may be seen from figure 17b that almost all the energy (compare with table 3 for stored energy) is dissipated in a discharge zone. Typical load voltage and currents waveforms from probes in the treatment chamber are given in figure 18 for the fragmentation regime at charging voltages 20 and 45 kV. Table 3 shows main parameters of the generator operation depended on the charging voltage. It may be seen from figure 18 that there is pronounced HV discharge phase with quasi-rectangular shape of the voltage pulse, in contrast with sharp voltage peak for the #1 generator. Table 3 demonstrates that duration of this HV phase decreases at the voltage increase. About 55% from the initial stored energy is dissipated in the discharge zone for this regime, the rest in the switches, internal capacitor resistances and another active elements of the discharge circuit.

5 Summary

An innovative design of repetitive pulsed generators for materials fragmentation has been successfully developed. Important features of the generators include: a) self contained system design;

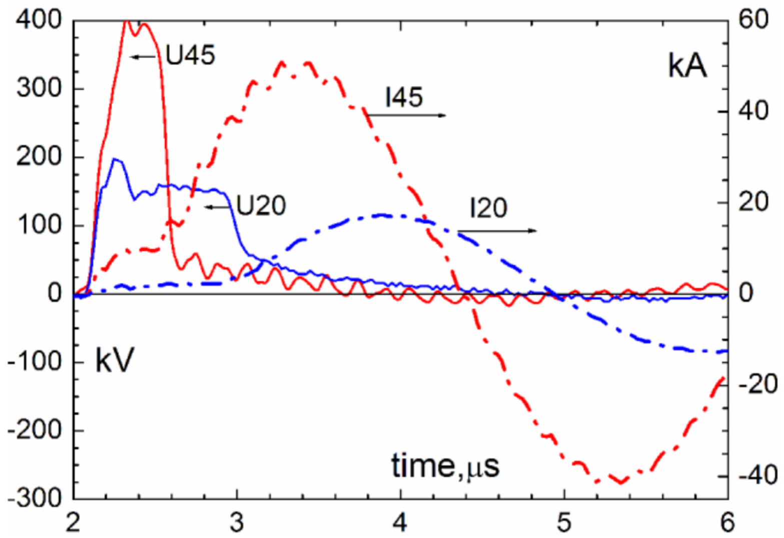

Figure 18. Waveforms of the load voltage (solid lines) and current (dash dot lines) for the fragmentation regime at charging voltages 20 and 45 kV.

Table 3. Summary of the generator tests results on rock load.

P	U	Stored energy (J)	Load voltage (kV)	Load current (kA)	HV phase duration (ns)
1	20	1280	190	17	1000
2	32	3277	280	34	800
2.5	39	4867	340	42	600
3	45	6480	410	51	500

b) compact configuration for easy set up in the lab; c) low EMI signature, to avoid interference with adjacent electronic equipment; d) intrinsically safe design with electrical interlocks for added protection of personnel; e) repetitive pulse operation for high productivity; f) sealed treatment chamber to isolate processing products. Only dry air is used as expendable material during operation for both generators. No failures have been observed in ~ 20000 test shots on each generator.

References

[1] S. Pronko, G. Schofield, M. Hamelin and F. Kitzinger, *Megajoule pulsed power experiments for plasma blasting mining applications*, *IEEE Int. Pulsed Power Conf.* **1** (1993) 15.

[2] S. Boev et al., *Destruction of granite and concrete in water with pulse electric discharges*, *IEEE Int. Pulsed Power Conf.* **2** (1999) 1369.

[3] H. Inoue, I.V. Lisitsyn, H. Akiyama and I. Nishizawa, *Drilling of hard rocks by pulsed power*, *IEEE Electr. Insul. Mag.* **16** (2000) 19.

[4] G.G. Kanaev et al., *A high-voltage pulse generator for electric-discharge technologies*, *Instrum. Exp. Tech.* **53** (2010) 95.

[5] B.V. Semkin, A.F. Usov and V.I. Kurets, *The principles of electric impulse destruction of materials*, Nauka, St. Petersburg Russia (1995).

[6] V.I. Kurets, A.F. Usov and V.A. Tsukerman, *Electric pulse disintegration of materials* (in Russian), Kol'sk. Nauchn. Tsentr RAN, Apatity Russia (2002).

[7] V.F. Vazhov, R.R. Gafarov, S.Y. Datskevich, M.Y. Zhurkov and V.M. Muratov, *Electric-pulse breakdown and the breakage of granite*, Tech. Phys. **55** (2010) 833.

[8] U. Andres, I. Timoshkin, J. Jirestig and H. Stallknecht, *Liberation of valuable inclusions in ores and slags by electrical pulses*, Powder Technol. **114** (2001) 40.

[9] U. Andres, *Dielectric separation of minerals*, J. Electrostat. **37** (1996) 227.

[10] H. Bluhm et al., *Application of pulsed HV discharges to material fragmentation and recycling*, IEEE Trans. Dielect. Electr. Insul. **7** (2000) 625.

[11] U. Andres, *Liberation study of apatite-nepheline ore comminuted by penetrating electrical discharges*, Int. J. Miner. Process. **4** (1977) 33.

[12] U. Andres, *Electrical disintegration of rock*, Miner. Process. Extr. M. **14** (1995) 87.

[13] E. Wang, F. Shi and E. Manlapig, *Pre-weakening of mineral ores by high voltage pulses*, Miner. Eng. **24** (2011) 455.

[14] E. Wang, F. Shi and E. Manlapig, *Mineral liberation by high voltage pulses and conventional comminution with same specific energy levels*, Miner. Eng. **27-28** (2012) 28.

[15] T.H. Martin, M. Williams and M. Kristiansen eds., *J.C. Martin on pulsed power*, Plenum, New York U.S.A. (1996), pg. 185.

[16] V.Y. Ushakov, V.F. Klimkin and S.M. Korobeynikov, *Impulse breakdown of liquids*, Springer, Berlin Germany (2007).

[17] P. Doiphode and S. Chaturvedi, *Minimization of energy input to fluids for rock-fracturing experiments*, J. Appl. Phys. **89** (2001) 6024.

[18] V.V. Burkin, N.S. Kuznetsova and V.V. Lopatin, *Dynamics of electro burst in solids: I. Power characteristics of electro burst*, J. Phys. **D 42** (2009) 185204.

[19] V.V. Burkin, N.S. Kuznetsova and V.V. Lopatin, *Dynamics of electro burst in solids: II. Characteristics of wave process*, J. Phys. **D 42** (2009) 235209.

[20] H. Bluhm, *Pulsed power systems: principles and applications*, Springer-Verlag, Berlin Germany (2006) pp. 288–305.

[21] J. Hammon, D. Hopwood, M. Ingram, M. Klatt and T. Tatman, *Electric pulse rock sample disaggregator*, IEEE Int. Pulsed Power Conf. **2** (2001) 1142.

[22] E. Dal Martello et al., *Electrical fragmentation as a novel route for the refinement of quartz raw materials for trace mineral impurities*, Powder Technol. **224** (2012) 209.

[23] SELFFRAG LAB product specification at http://www.selfrag.com/pdf/products_specifications/tech-specification.pdf.

[24] B.M. Kovalchuk et al., *High-voltage pulsed generator for dynamic fragmentation of rocks*, Rev. Sci. Instrum. **81** (2010) 103506.